Electronic Supplementary Material (ESI) for RSC Advances.

Supporting information

Improved photocatalytic activity of g-C_3N_4 derived from cyanamide-urea solution

Xiangqian Fan,[a] Zheng Xing,[b] Zhu Shu,[c] Lingxia Zhang*[a], Lianzhou Wang,[b] Jianlin Shi*[a]

[a]State Key Laboratory of High Performance Ceramics and Superfine Microstructure, Shanghai Institute of Ceramics, Chinese Academy of Sciences, Shanghai 20050, PR China.

[b]ARC Centre of Excellence for functional Nanomaterials, School of Chemical Engineering, The University of Queensland, Brisbane, QLD 4072, Australia.

[c]Faculty of Material Science and Chemistry, China University of Geosciences, Wuhan 430074, PR China.

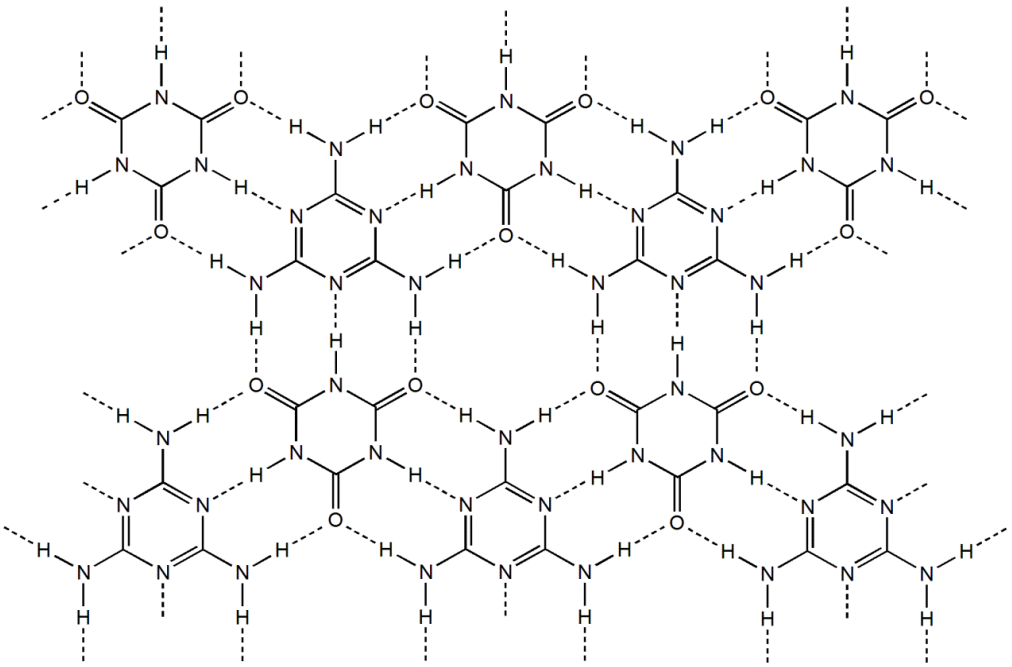

Figure S1. The structure model of melamine-cyanuric acid (MCA) complex

Table S1 Yield and elemental composition of the obtained g-C_3N_4 at different temperatures.

Sample	Yield [a] / g	C / wt%	N / wt%	H / wt%	C/N [b]
CN-500	3.48	33.03	56.47	2.44	0.68
CN-550	3.18	33.99	57.68	2.03	0.69
CN-600	3.05	34.51	57.80	1.81	0.70
CN-650	2.76	35.10	58.27	1.70	0.70
CN-700	1.44	35.63	58.91	1.60	0.71

[a] obtained from solution containing 5 g cyanamide and 2.5 g urea; [b] molar ratio.

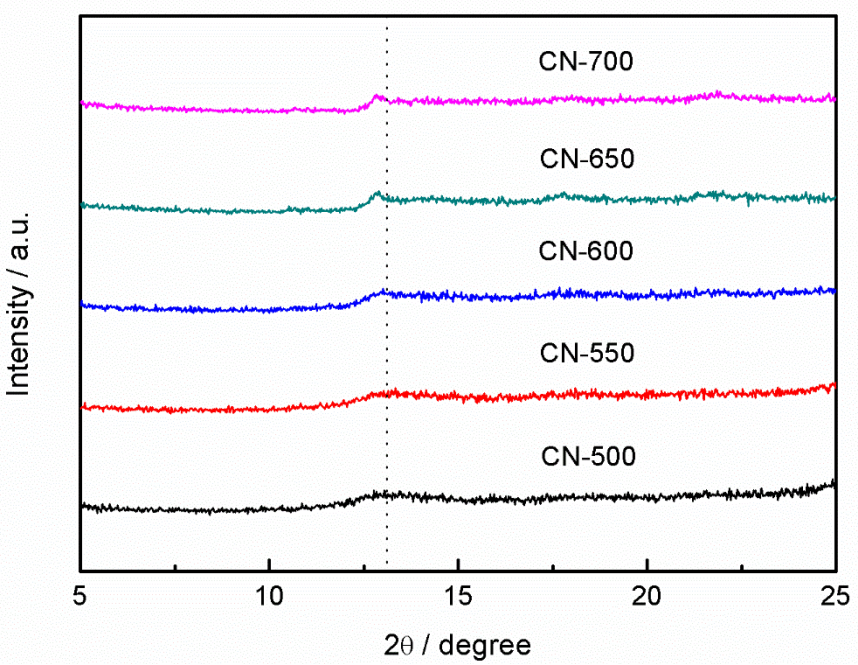

Figure S2. Enlarged XRD patterns (from 5°-25°) of g-C_3N_4 samples prepared at different temperatures.

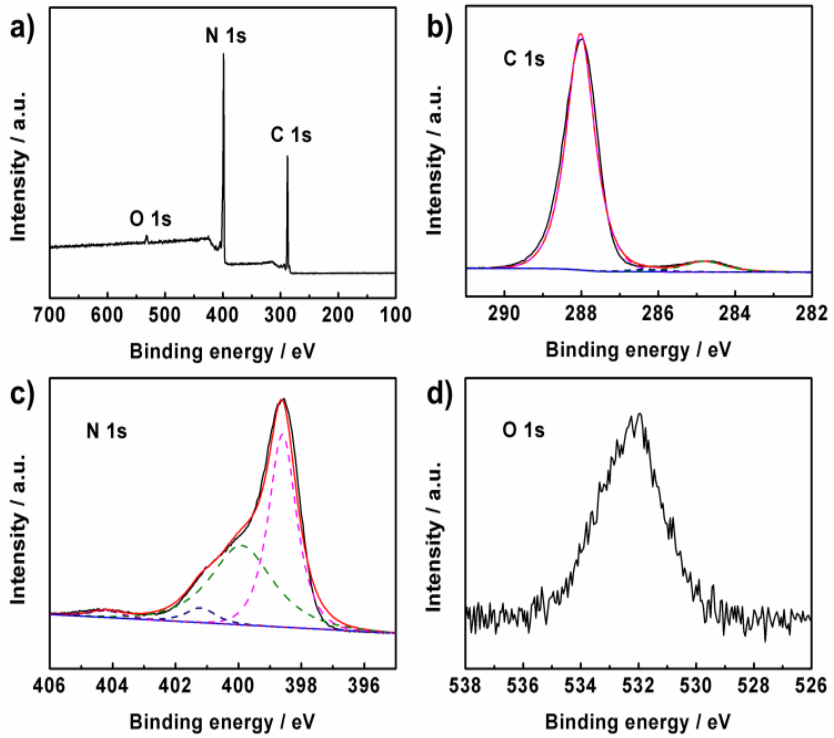

Figure S3. XPS spectrum of CN-700 (a) and the corresponding high resolution spectra of C 1s (b), N 1s (c) and O 1s (d).

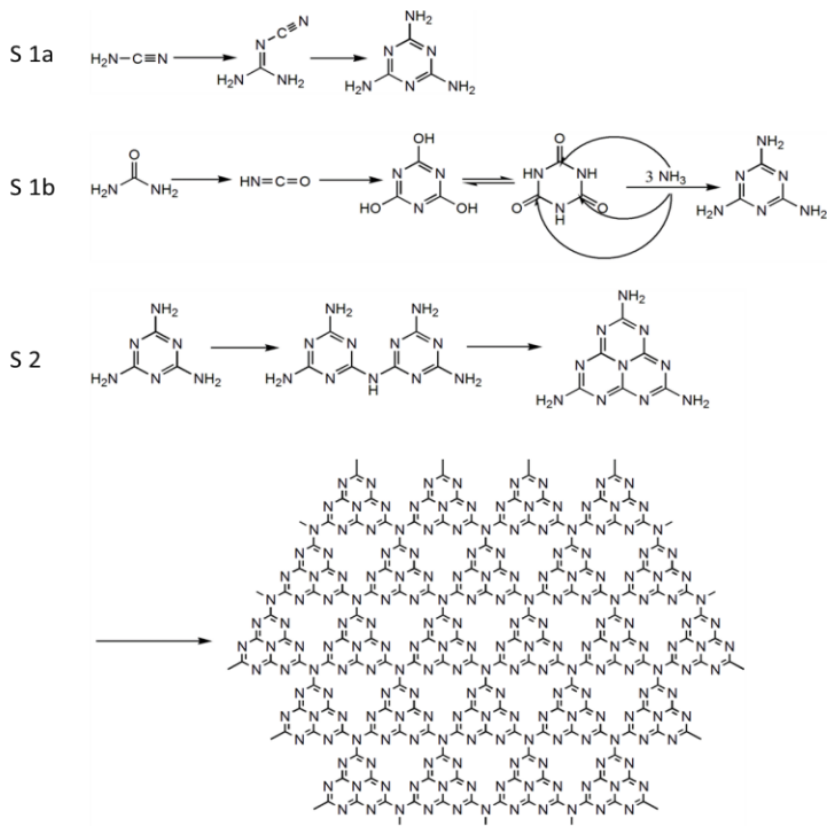

Scheme S1. The possible reaction path for the formation of g-C_3N_4 from cyanamide-urea solution . S: the reaction step.

Table S2 Physicochemical properties and photocatalytic activity of the obtained g-C_3N_4 for H_2 evolution under visible light.

Sample	S_{BET} / m^2 g^{-1}	Band gap[a] / eV	HER [b] /μmolh^{-1}
g-C_3N_4[c]	8.0	2.70	9.6
CN-500	3.0	2.74	5.0
CN-550	5.8	2.70	5.5
CN-600	15.3	2.65	9.4
CN-650	29.3	2.93	22.8
CN-700	36.3	3.01	32.4

[a] estimated by optical measurements. [b] H_2 evolution rate. [c] synthesized by cyanamide polymerization.

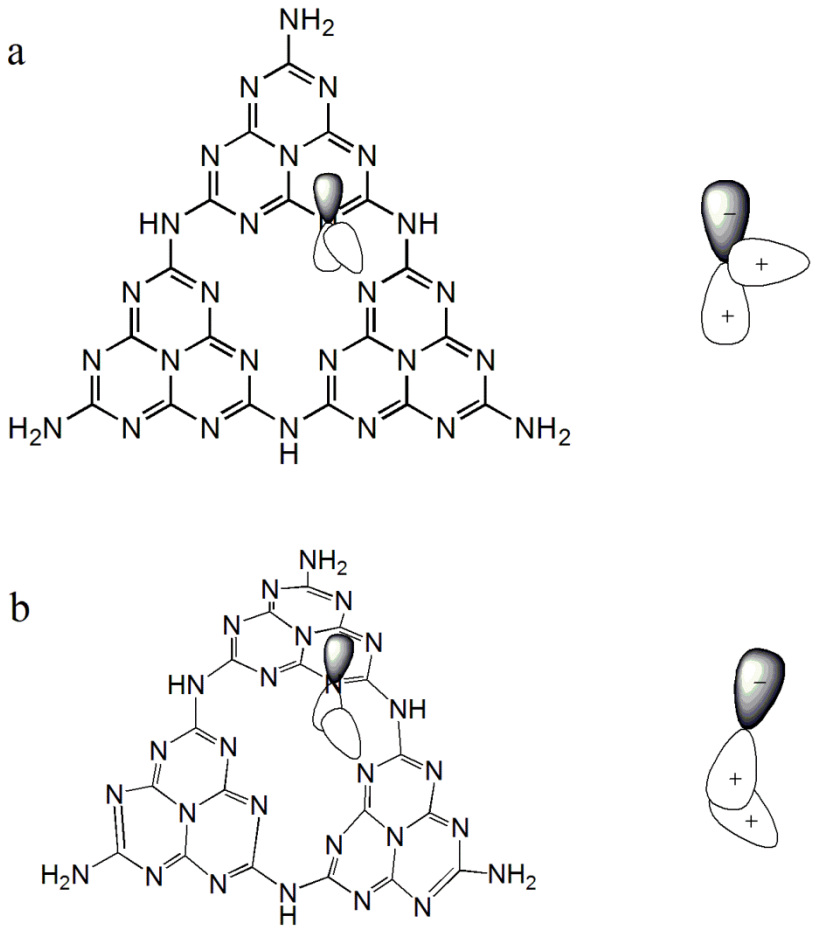

Figure S4. Overlap situations between p orbital and n orbital of (a) completely planarized g-C_3N_4;(b) incompletely planarized g-C_3N_4.

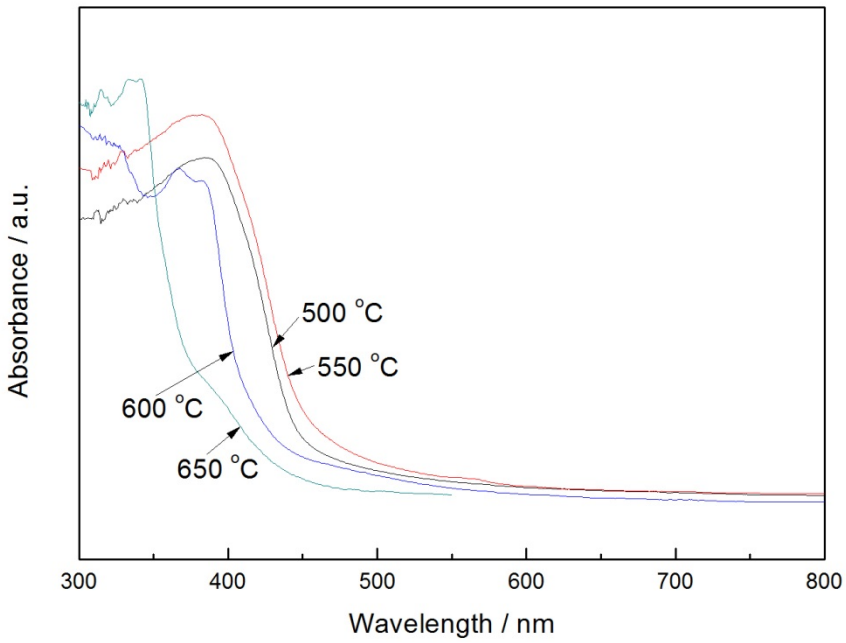

Figure S5. The UV-Vis diffuse reflectance absorption spectra of melamine-derived g-C_3N_4 obtained at different temperatures.

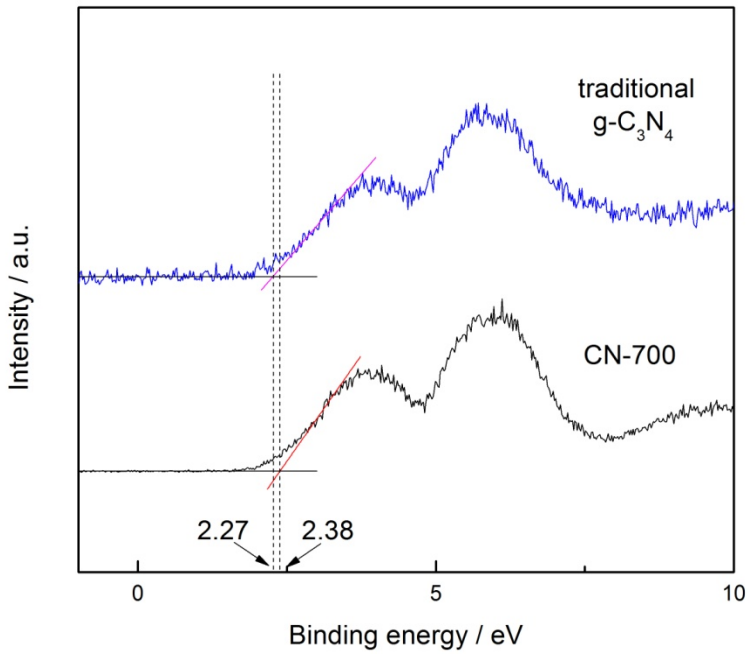

Figure S6. Valence band XPS spectra of traditional g-C_3N_4 and CN-700.

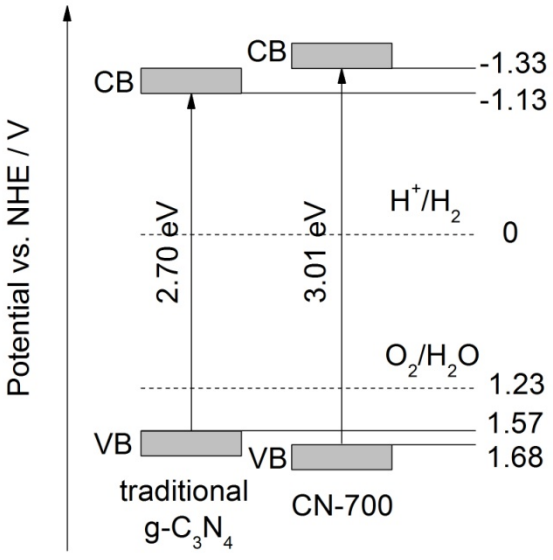

Figure S7. Electronic potential diagrams for traditional g-C_3N_4 and CN-700.

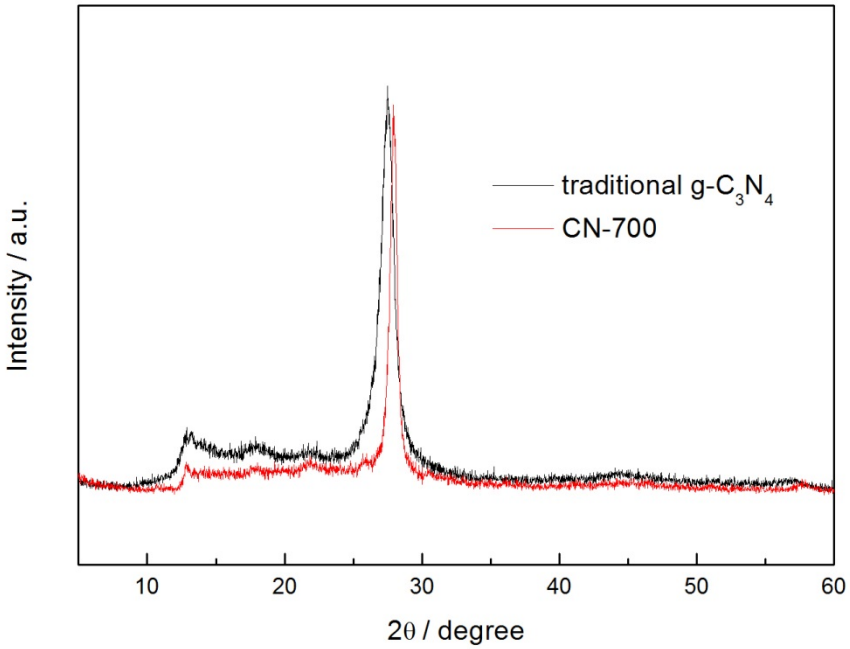

Figure S8. XRD patterns of traditional g-C_3N_4 and CN-700.

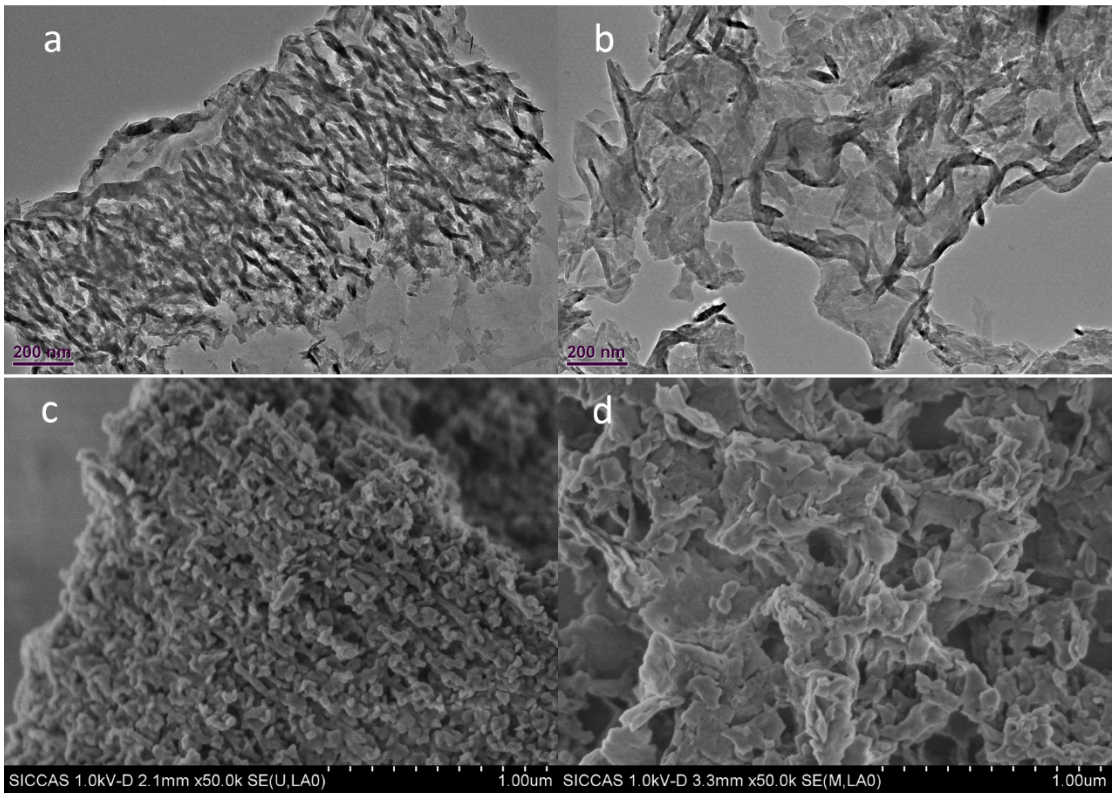

Figure S9. Typical TEM and SEM images of traditional g-C_3N_4 (a and c,respectively) and CN-700 (b and d, respectively).